High Resolution Electromechanical Imaging of Ferroelectric Materials in a Liquid Environment by Piezoresponse Force Microscopy

Brian J. Rodriguez, Stephen Jesse, A. P. Baddorf, and Sergei V. Kalinin*

Materials Science and Technology Division, Oak Ridge National Laboratory, Oak Ridge, Tennessee 37831, USA

(Received 19 January 2006; published 16 June 2006)

High-resolution imaging of ferroelectric materials using piezoresponse force microscopy (PFM) is demonstrated in an aqueous environment. The elimination of both long-range electrostatic forces and capillary interactions results in a localization of the ac field to the tip-surface junction and allows the tip-surface contact area to be controlled. This approach results in spatial resolutions approaching the limit of the intrinsic domain-wall width. Imaging at frequencies corresponding to high-order cantilever resonances minimizes the viscous damping and added mass effects on cantilever dynamics and allows sensitivities comparable to ambient conditions. PFM in liquids will provide novel opportunities for high-resolution studies of ferroelectric materials, imaging of soft polymer materials, and imaging of biological systems in physiological environments on, ultimately, the molecular level.

DOI: 10.1103/PhysRevLett.96.237602 PACS numbers: 77.80.Fm, 68.37.−d, 77.65.−j

Electromechanical coupling is ubiquitous among inorganic materials and biological systems. In the latter case, piezoelectricity is linked to physiological structure and biochemical functionality. The combination of polar bonding and optical activity results in a piezoelectric response comparable to quartz ($\sim$ 1–3 pm/V) in virtually all biopolymers [1]. The ability to probe electromechanical coupling on the molecular scale in living biosystems will improve the understanding of piezoelectric biofunctionality and pave the way for advances in molecular electromechanical systems.

A key tool for probing electromechanical coupling on the nanoscale is piezoresponse force microscopy (PFM), which is based on the direct measurement of local electromechanical coupling in a piezoelectric material using a periodically biased atomic force microscope (AFM) tip [2,3]. PFM has been established as a powerful tool for investigating low-dimensional ferroelectrics for nonvolatile memory devices [4,5] and data storage applications [6,7]. A number of recent advances have been enabled by PFM, including the identification of the origins of ferroelectricity in ferroic superlattices [8,9], the mechanisms of magnetoelectric coupling and polarization switching in multiferroic nanostructures [10], the statistical physics of domain walls in ferroelectrics [11], and the structure of polar nanodomains in ferroelectric relaxors [12]. Recent improvements in PFM sensitivity have permitted the investigation of a wide variety of weakly piezoelectric materials such as III-nitride thin films [13] and biopolymers in calcified and connective tissues [14,15] with up to 10 nm resolution. However, in order to address electromechanical phenomena in biological systems, probe electroactive soft condensed matter systems, and perform high-resolution studies of ferroelectric perovskites, a fundamentally different approach to PFM is required that minimizes both the electrostatic interactions and the tip-surface forces. Here, we explore PFM imaging in a liquid environment [16] as a means to control these detrimental mechanisms [17] and ultimately probe electromechanical coupling on the molecular level. The successful demonstration of liquid electromechanical imaging on a model ferroelectric system enables these future studies.

Achieving the goal of single-molecule electromechanical imaging in liquids requires an improvement in the resolution and sensitivity of PFM, ideally to the subnanometer level in ferroelectric perovskites and to the molecular level in ferro- and piezoelectric polymers. Three factors limiting the resolution of PFM are (a) electrostatic contributions to the signal, (b) large (>100 nN) tip-surface forces present in contact mode imaging, and (c) capillary forces due to condensed atmospheric moisture. The quadratic bias dependence of electrostatic forces on the cantilever present during PFM measurements does not allow the electromechanical response, which has a linear bias dependence, to be distinguished unambiguously from the electrostatics. The electrostatic effects can be minimized by using stiff cantilevers, but at the expense of larger indentation forces and reduced resolution [18].

Liquid PFM was implemented on a commercial AFM system (Veeco MultiMode NS-IIIA) equipped with additional function generators and lock-in amplifiers (DS 345, SRS 830, and SRS 844, Stanford Research Instruments, and Model 7280, Signal Recovery) and an external signal generation and data acquisition system. A custom-modified commercial liquid cell (Veeco) was used to bias the tip directly during contact mode operation in liquid. Measurements were performed using Au coated Si tips (Micromasch, spring constant $k \sim 0.3$ N/m). Electromechanical imaging of a model polycrystalline lead zirconate-titanate (PZT) ceramics (95:5 Zr/Ti composition) was performed in distilled water and NaCl solutions. As in air, liquid PFM measurements were performed by applying a modulation voltage to a tip in contact with a piezoelectric surface. The electric field generated at the tip-

surface junction deforms the piezoelectric surface, thereby deflecting the tip. The amplitude and phase of the tip oscillation were recorded simultaneously with surface topography. The PFM amplitude is proportional to the tip deflection (surface displacement) while the phase contains information about the orientation of the polarization of the material beneath the tip.

Shown in Fig. 1 are surface topography, PFM amplitude, and PFM phase images of PZT acquired in distilled water at 629 kHz. The topographic structure is related to the domain orientation as revealed by preferential etching. The amplitude images exhibit greater signal strength at the center of the domains with characteristic minima at the domain walls. The phase signal changes by 180° at the domain walls, indicative of reliable PFM contrast. Remarkably, the resolution in liquid PFM images is appreciably larger than in ambient PFM. To quantify the resolution, the domain-wall profile has been fit to the function $R(x) = R_- + (R_+ - R_-)\tanh[(x - x_0)/(w/2)]$, where R_+ (R_-) is the response on the left (right) of the domain wall centered at x_0 and w is the width of the domain wall [19]. For some domain walls, the widths were as small as ~3 nm, i.e., close to the intrinsic domain-wall width (several unit cells, 1–1.5 nm) of the ferroelectric. In comparison, domain-wall widths observed under ambient conditions were typically ~30 nm. The resolution in the phase signal also improved from 2 nm in ambient to 0.2 nm in liquid.

Force-distance and PFM signal-distance curves are shown in Figs. 2(a) and 2(b). Note the complete absence of any measurable capillary hysteresis in liquid [Fig. 2(b)] as compared to ambient [Fig. 2(a)] due to the absence of liquid necks and reduced van der Waals interactions. PFM amplitude and phase images obtained at various positions along the force-distance curve are shown in Fig. 2. Note that, while the PFM contrast is virtually constant for indentation forces from 48 to 18 nN, the signal rapidly decreases from 3 to 0 nN and disappears at −4.5 nN, corresponding to a loss of tip-surface contact. In comparison, in ambient PFM, an increase in the tip-surface separation results in a marked discontinuity between an electromechanical (in contact) to a purely electrostatic (noncontact) behavior [20]. Any electrostatic contrast apparent under ambient conditions in the noncontact regime is absent when imaging in liquid.

The dynamic behavior of the cantilever was investigated using amplitude-frequency and amplitude-bias spectroscopy as illustrated in Fig. 3(a). At low frequencies, the PFM response in liquid is reduced by more than an order of magnitude as compared to ambient and the first resonant peak is shifted (from 83.64 to 217.77 kHz) and damped ($Q = 7$ in liquid vs 20 in air). For high-order resonances, the Q factor increases, achieving $Q_i = 13.6$ for $i = 3$. This is due to a reduction in the volume of liquid excited by the cantilever at higher-order resonances and results in diminished viscous damping [21]. In particular, the maximum signal at the second resonance in liquid is within a factor of 2 of the 1st ambient resonance. Thus, resonant enhancement at high-order modes in liquid is possible and the measured sensitivity is comparable to that in ambient. The PFM signal was also measured as a function of dc tip bias. The amplitude-frequency response curves do not change when a dc bias is applied to the tip indicating the absence of an electrostatic contribution to the signal [22].

To determine the effects of the Debye length on the PFM signal amplitude, i.e., the screening range of the electrostatic forces in the solution, PFM imaging and amplitude-

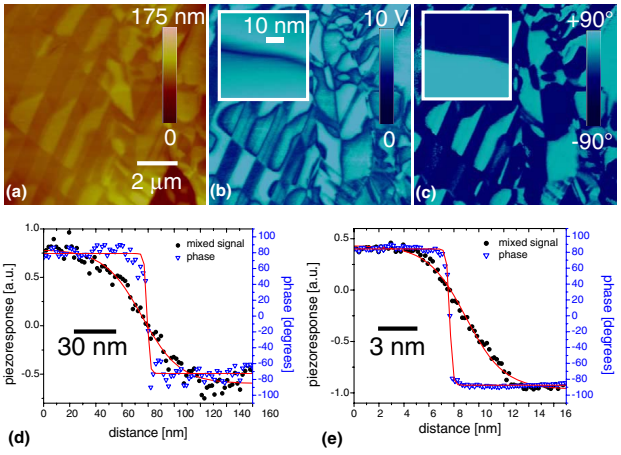

FIG. 1 (color online). (a) Surface topography and PFM (b) amplitude and (c) phase images of PZT acquired in distilled water at 10 V. The PFM amplitude is a measure of the piezoelectric response of the material, while the PFM phase signal contains information on the orientation of the material. PFM mixed signal and phase profile across a typical domain wall in (d) ambient and (e) liquid environments. Note the order of magnitude increase in resolution.

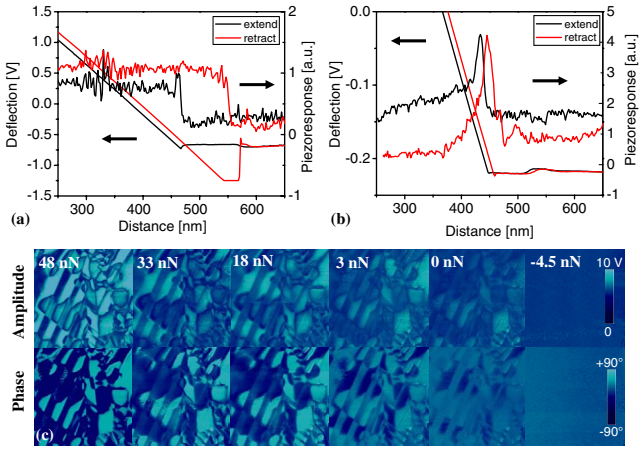

FIG. 2 (color online). Force-distance curves and distance dependence of PFM signal in (a) ambient and (b) liquid environments (10 V, 624 kHz). Note the absence of capillary hysteresis in liquid in the plot of deflection vs distance (force-distance curve) in (b). (c) A series of PFM amplitude (top) and phase (bottom) images obtained at different loading forces. The contrast decreases above the surface.

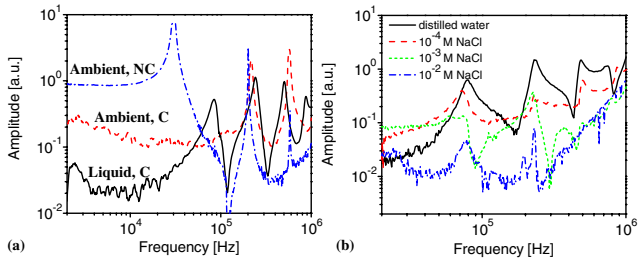

FIG. 3 (color online). (a) PFM signal amplitude-frequency curves in ambient contact (C) and noncontact (NC) regimes and in liquid contact. (b) PFM amplitude-frequency response for different NaCl concentrations.

frequency spectroscopy were performed in NaCl solutions with concentrations of 10^{-4}, 10^{-3}, 10^{-2}, and 10^{-1} M. The corresponding Debye lengths, $\lambda_D = \sqrt{\varepsilon\varepsilon_0 k_B T/ce^2} = 0.304/\sqrt{c}$ nm (for 1:1 electrolytes), are 30.4, 9.6, 3.04, and 0.96 nm. The relaxation frequency (1.8 MHz for a 10^{-4} M NaCl solution) is sufficiently high to ensure efficient screening. PFM images for various salt concentrations (not shown) exhibit robust PFM contrast in a 10^{-4} M solution, contrast deterioration in 10^{-3} and 10^{-2} M solutions, and no contrast in the 10^{-1} M solution. The corresponding PFM amplitude-frequency curves for a cantilever in solutions with varying salt concentrations are illustrated in Fig. 3(b).

From these observations, the following picture of PFM imaging in liquid vs ambient environment emerges. In an ambient environment, the tip interacts with the surface through electrostatic forces and short-range electromechanical interactions. The piezoresponse (PR) signal, i.e., the first harmonic component of tip oscillation induced by a periodic bias applied to the tip, is

$$\mathrm{PR} = \mathrm{PR}_{\mathrm{em}} + \mathrm{PR}_{\mathrm{el}}, \tag{1}$$

In the low-frequency limit, the electromechanical response is [22]

$$\mathrm{PR}_{\mathrm{em}} = \alpha_a(h)\tilde{d}_{33}\frac{k_1}{k_1 + k}, \tag{2}$$

where $\tilde{d}_{33}$ is the electromechanical response of material, $\alpha_a(h)$ is the ratio of the ac tip potential to the ac surface potential of the ferroelectric (i.e., the potential drop in the tip-surface gap), k_1 is the spring constant of the tip-surface junction, and k is the spring constant of the cantilever. In ambient or vacuum, the electrostatic forces are long range, $F_{\mathrm{el}}^{\mathrm{amb}} = (1/2)C_z'(z)(V_t - V_s)^2$, where V_t is the tip potential, V_s is the surface potential, and $C_z'(z)$ is the tip-surface capacitance gradient. The electrostatic contribution is thus

$$\mathrm{PR}_{\mathrm{el}}^{\mathrm{amb}} = \left(\frac{C'_{\mathrm{sphere}} + C'_{\mathrm{cone}}}{k_1 + k} + \frac{C'_{\mathrm{cant}}}{24k}\right)(V_{\mathrm{dc}} - V_s), \tag{3}$$

where C'_{sphere}, C'_{cone}, and C'_{cant} are the capacitance gradients due to the spherical and conical parts of the tip and cantilever, respectively [22]. V_{dc} is the dc potential offset of the tip bias, and h is the tip-surface separation. In a sphere-plane model for small separations, $C'_{\mathrm{sphere}}(h) = \pi\varepsilon_0 R/h$, where R is the tip radius of curvature. In ambient, $\alpha_a(h) = 1$ for $h < 0$ (contact), i.e., the response is independent of the penetration depth [23] and $\alpha_a(h) \ll 1$ for $h > 0$ (noncontact), giving rise to the well-known limits of PFM and Kelvin probe force microscopy. As shown in Figs. 4(a) and 4(b), the capacitive tip-surface electrostatic interaction is present for both noncontact and contact modes of operation. However, the electromechanical coupling is present only in the contact mode [double arrow in Fig. 4(b)].

In liquid, the PFM contrast is strongly mediated by the presence of mobile ions that screen electrostatic tip-surface interactions. For the sphere-plane system [24]

$$F_{\mathrm{el}}^{l}(z) = \frac{\varepsilon\varepsilon_0 R}{\lambda_D}\frac{2V_tV_s\exp(h/\lambda_D) - (V_t^2 + V_s^2)}{\exp(2h/\lambda_D) - 1}. \tag{4}$$

Electrostatic interaction in liquid is short-range due to screening by mobile ions and decays exponentially for $h > \lambda_D$ [Figs. 4(c) and 4(d)]. Thus, the electrostatic contribution to the PFM signal in liquid is (for $h > 0$)

$$\mathrm{PR}_{\mathrm{el}}^{\mathrm{liq}} = \frac{\varepsilon\varepsilon_0 R}{\lambda_D}\frac{2V_s\exp(h/\lambda_D)}{\exp(2h/\lambda_D) - 1}\frac{1}{k_1^l + k}, \tag{5}$$

where k_1^l is tip-surface spring constant in liquid. The contribution from the conical part of the tip and cantilever is absent for $R \gg \lambda_D$. Note that the increase in response observed at the contact point in liquid [Fig. 2(b)] is due to additional electrostatic coupling in the double layer. The response decreases with increasing force due to the increased contact stiffness.

The electromechanical response in liquid is described by Eq. (2), where the tip-surface spring constant now includes the effect of the liquid layer. The screening coefficient is

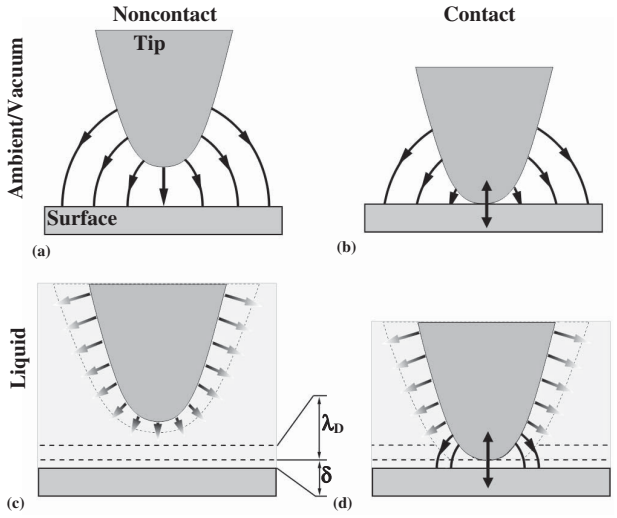

FIG. 4. Schematic mechanism of PFM contrast enhancement in a liquid environment. In ambient (a),(b) electrostatic forces are present between the tip and the sample. Electromechanical coupling (double arrow) is present only for the contact mode, when tip and surface are in contact. In liquid (c),(d) the electrostatic forces are minimized.

$\alpha(h) = 1$ in Eq. (2) for $h \ll \lambda_D$, i.e., when the tip touches the surface, and is $\alpha(h) = 0$ if the electric double layers around the tip and the surface do not overlap. Thus, the electromechanical response [Eq. (2)] in solution gradually decays at distances on the order of the Debye length of the solution, and the electrostatic contribution is reduced as compared to ambient imaging [Fig. 4(d)].

The absence of PFM contrast in high concentrations of NaCl and the stiffening of the tip-surface contact for high indentation forces suggest that in liquid PFM the tip is separated from the surface by a liquid layer of thickness $\delta \sim 1$–3 nm formed due to interactions between the hydrophobic gold tip and the hydrophilic PZT surface [25,26]. The PFM contrast disappears for $\lambda_D \ll \delta$, i.e., at high NaCl solution concentrations. The thickness, δ, provides a lower boundary for PFM resolution. The presence of the water layer also prevents the transfer of in-plane sample oscillations to the tip via tip torsion and, indeed, no lateral PFM signal was detected.

To summarize, we have demonstrated electromechanical imaging in a liquid environment with ~ 3 nm resolution and elucidated the image formation mechanisms. The mobile ions present in the solution effectively screen the long-range electrostatic interactions at distances greater than the Debye length, thus localizing the ac field to the tip-surface junction. This novel mechanism of electromechanical tip-surface interactions enables high spatial resolutions approaching the intrinsic ferroelectric domain-wall width limit. It is shown that electromechanical imaging using high (> 2) order cantilever resonances minimizes both the added mass and hydrodynamic damping effects on cantilever dynamics, and provides a signal level comparable to ambient conditions. The elimination of capillary interactions and the control of van der Waals tip-surface forces in a liquid environment allow precise control of tip-surface separation and contact stiffnesses, which are essential for successful molecular-resolution imaging. We believe that electromechanical imaging in liquids is the key to achieving domain-wall width resolutions in perovskites and molecular resolution in soft polymers and biological systems.

Support from ORNL SEED funding under Contract No. DE-AC05-00OR22725 (B. J. R., S. V. K.) and from the NIH National Human Genome Research Institute under Grant No. R01 HG002647 through the University of North Carolina (S. J., A. P. B.) is acknowledged. The authors are grateful to E. W. Plummer and H. H. Weitering for insightful comments and useful discussion. PZT sample courtesy of Chad Watson, Sandia National Laboratories.

*Corresponding author.
Electronic address: sergei2@ornl.gov

[1] E. Fukada, Biorheology **32**, 593 (1995).
[2] P. Güthner, J. Glatz-Reichenbach, and K. Dransfeld, J. Appl. Phys. **69**, 7895 (1991).
[3] *Nanoscale Characterization of Ferroelectric Materials*, edited by M. Alexe and A. Gruverman (Springer, Berlin, Germany, 2004).
[4] J. Scott, *Ferroelectric Memories* (Springer Verlag, Berlin, 2000).
[5] *Nanoelectronics and Information Technology*, edited by R. Waser (Wiley-VCH, New York, 2003).
[6] T. Tybell, C. H. Ahn, and J.-M. Triscone, Appl. Phys. Lett. **72**, 1454 (1998).
[7] T. Tybell, P. Paruch, T. Giamarchi, and J.-M. Triscone, Phys. Rev. Lett. **89**, 097601 (2002).
[8] M. Dawber, C. Lichtensteiger, M. Cantoni, M. Veithen, P. Ghosez, K. Johnston, K. M. Rabe, and J.-M. Triscone, Phys. Rev. Lett. **95**, 177601 (2005).
[9] C. H. Ahn, K. M. Rabe, and J.-M. Triscone, Science **303**, 488 (2004).
[10] J. Wang, J. B. Neaton, H. Zheng, V. Nagarajan, S. B. Ogale, B. Liu, D. Viehland, V. Vaithyanathan, D. G. Schlom, U. V. Waghmare, N. A. Spaldin, K. M. Rabe, M. Wuttig, and R. Ramesh, Science **299**, 1719 (2003).
[11] P. Paruch, T. Giamarchi, and J.-M. Triscone, Phys. Rev. Lett. **94**, 197601 (2005).
[12] V. V. Shvartsman and A. L. Kholkin, Phys. Rev. B **69**, 014102 (2004).
[13] B. J. Rodriguez, A. Gruverman, A. I. Kingon, R. J. Nemanich, and O. Ambacher, Appl. Phys. Lett. **80**, 4166 (2002).
[14] C. Halperin, S. Mutchnik, A. Agronin, M. Molotskii, P. Urenski, M. Salai, and G. Rosenman, Nano Lett. **4**, 1253 (2004).
[15] S. V. Kalinin, B. J. Rodriguez, S. Jesse, T. Thundat, and A. Gruverman, Appl. Phys. Lett. **87**, 053901 (2005).
[16] The only published attempt for PFM in liquid is by Ganpule, when a highly conductive liquid was used as a top electrode, C. Ganpule, Ph.D. thesis, University of Maryland, College Park, 2001.
[17] H. J. Butt, B. Capella, and M. Kappl, Surf. Sci. Rep. **59**, 1 (2005).
[18] *Nanoscale Characterization of Ferroelectric Materials*, edited by M. Alexe and A. Gruverman (Springer, Berlin, Germany, 2004).
[19] M. Bode, Rep. Prog. Phys. **66**, 523 (2003); A. Hubert and R. Schäfer, *Magnetic Domains* (Springer, Berlin, 1998).
[20] S. V. Kalinin and D. A. Bonnell, Phys. Rev. B **63**, 125411 (2001).
[21] C. P. Green and J. E. Sader, J. Appl. Phys. **98**, 114913 (2005).
[22] S. Jesse, A. P. Baddorf, and S. V. Kalinin, Nanotechnology **17**, 1615 (2006).
[23] S. V. Kalinin, E. Karapetian, and M. Kachanov, Phys. Rev. B **70**, 184101 (2004).
[24] W. R. Bowen, A. N. Filippov, A. O. Sharif, and V. M. Starov, Adv. Colloid Interface Sci. **81**, 35 (1999).
[25] G. A. Kimmel, N. G. Petrik, Z. Dohnálek, and B. D. Kay, Phys. Rev. Lett. **95**, 166102 (2005).
[26] J. Israelachvili, *Intermolecular and Surface Forces* (Academic, San Diego, 1991).